LUCY, A CRT FILM MEASURING DEVICE - A BRIEF DESCRIPTION OF THE PROTOTYPE AND RESULTS OF DETAILED HARDWARE PERFORMANCE MEASUREMENTS

H. Anders, D. Jacobs, W. Krischer, A. Lewis*),
T. Lingjaerde, D. Lord, J. Oropesa, A. van Praag,
B. Stumpe, L. Turek**), D. Wiskott and R. Zurbuchen

CERN, Geneva, Switzerland

1. Introduction

In designing LUCY it was attempted to attain the current technical limits of a computer controlled CRT measuring device for track chamber film. The system was chosen to give the highest possible accuracy and stability combined with a large degree of flexibility. In fact, the aim was to obtain the precision and stability of the HPDs and make use of the flexibility offered by a CRT.

To achieve this objective the following principles have been adopted:

i) Very great care has been taken in the design or selection of all mechanical, optical and electronic parts.

ii) Only a flying spot and not a line is used.

iii) The spot is continuously under digital control, even during the movement along the scan lines.

iv) To cover rectangular formats a precision film stage was developed which can be moved rapidly and precisely in the longitudinal direction to provide access to the different parts of one frame.

---

*) On leave from AERE, Harwell, England.

**) On leave from Instytut Badan Jadrowych 2 V1, Al Mickiewicza 30, Krakow, Poland.

A prototype of this system has been constructed as a single view machine. It has a very fast film transport suitable for the formats 35, 50 and 70 mm × 210 mm perforated and non-perforated on rolls of up to 300 m.

Detailed measurements have been carried out on this prototype to establish a solid basis for a future measuring system.

In the following sections a brief description of the system will be given. Then the results of the test measurements will be presented and tentatively extrapolated to other formats and the low contrast film from BEBC.

2. General description of the system

Figure 1 shows a block diagram of the system. It is controlled by a PDP 9 computer which sets up the parameters of the scan. Special purpose digital hardware controls the movement of the spot via the X and Y deflection amplifiers. Static and dynamic focus and astigmatism corrections are provided. Linearity correction is performed by analogue circuits.

A 7" Ferranti tetrode CRT is foreseen but the tube mount can take a 9" tube with only minor modifications. The output of the photomultiplier first undergoes compensation for variations of the CRT light output. After filtering by a $\sin^2$-filter, track pulses are generated by the track detector. The track pulses are digitized and, after buffering, sent to the PDP9 via the DMA channel.

The computer also controls the movement of the film transport and the film gate and reads their positions.

There are four displays: two storage scopes for digital information, one scan monitor which shows the actual position of the spot and a video monitor for analogue display of the tracks detected by the video amplifier.

As mentioned above, the film gate can be displaced rapidly to provide access to different parts of a rectangular picture of up to 70 mm wide and 210 mm long. At one extreme position of the gate a calibration grid is in the scanning area. In this position the film can be optically projected on to a viewing screen.

All parts indicated on the block diagram are ready, apart from the dynamic astigmatism and linearity correction and the final video amplifier which are under development.

3. Area raster scan

The spot on the CRT is controlled in X and Y directions by digital counters, whose resolution is 1:16000. Within this coordinate system the spot can perform area scans, the parameters of which are under computer control.

The spot is first addressed to a certain coordinate by presetting the counters. From this point scan lines of any length are drawn in X or Y by incrementing the counter, which is selected to be the "fast" one, at a rate of 5 MHz. At the end of one line the other counter, the "slow" one, is incremented and another line started. Thus an area raster scan is drawn, whose number of scan lines, scan line spacing, scan line length and orientation in X or Y are preset every time by the computer. The area scan can be given the shape of a parallelogram by shifting the starting points of the lines. The angle of the parallelogram can be varied in steps of about 0.5°.

The movement of the spot does not follow the individual fast steps of 1:16000 but is continuous. Therefore interpolation can be used and a least count of 1:65000 has been selected. The D/A converter has in fact a correspondingly high stability.

4. The measurements

There are two groups of measurements. The first are over-all measurements with the spot under computer control and digitizings returned to the computer. The second group was made to examine the properties of the spot and the resolution,using test grids and real film. Two tubes of the same type, Ferranti 7/75 gun, were examined, one with phosphor type A and the other with phosphor type Q4.

5. Over-all measurements

Figure 2 gives a list of the results of the over-all measurements. The numbers in the last column indicate the figure numbers in which the details of these measurements are given.

Figure 3 shows the distribution of the digitizings if one scan line is repeated about 300 times. For comparison, values measured on HPD II are added (see CERN report 68-4). Both measurements were made on the same grid line.

The histogram presented on Fig. 4 was produced under the same conditions, but using instead a typical 2m HBC track. In Fig. 5 the scatter of the digitizings along a track as a function of the angle with the scan line is plotted. It shows the original plot from the HPD II report (CERN report No. 68-4) to which the two values found with LUCY have been added. It can be seen that they are not inferior to those of the HPD.

Figure 6 shows the scatter of the digitizings on a 35 mm long track after fitting to a 5th order polynomial and digital filtering.

Figure 7 demonstrates that the scatter of the digitizings is independent of the position of the screen. Sixty-four crosses of the calibration grid, distributed evenly over the screen, have been taken as fiducial marks. A straight line has been fitted to the digitizings of each arm of the crosses. The r.m.s. deviation from these straight lines is within 2 μm over the whole area. In this connection it must be mentioned that, due to the fact that no linearity correction was applied to the scan, the fit to a straight line is made less precise.

Figure 8 demonstrates the long term stability of the system. The positions of 16 fiducial crosses spread over the measuring area were measured in a period of 16 hours. The plot shows the displacement of the individual cross centres. It is seen that the displacement found does not exceed the measuring error of 5μm.

The results of a preliminary calibration are shown in Fig. 9.

The measurements of the scan delay presented in Fig. 10 prove that at constant scan speed the scan delay in the middle of the field does not differ from the values measured at the edges by more than the equivalent of 1.6 μm. This excludes the need for position dependent corrections to the digitizings when the scan line direction is reversed.

6. Extrapolation of the measurements to other formats

The measurements listed in Fig. 2 were made on a 50 × 50 mm^2 film area using a demagnification of 2:1. A rough extrapolation to other magnifications of the reproducibility of single hits and of the scatter on tracks has been tried. In doing this, two simplifying assumptions have been made.

i) It is supposed that the present film plane spot size can be maintained at the larger magnifications. This is possible if a tube with phosphor A is used, giving a smaller spot on the tube face, and if careful dynamic astigmatism corrections are made.

ii) The track images are assumed to be the same in each case. The effect of small, low contrast bubbles is discussed in the next section.

The scatter of digitizings on a track comes from several sources; the natural scatter of the bubbles about the centre, the effect of jitter of the spot on the CRT screen and the effect of electrical noise on the video signal. The last is a function of the angle at which the scan lines cross the track. Of these sources only the effect of spot jitter changes with magnification. The contributions from each source in the present tests have been calculated from the results as follows. Firstly, it has been assumed (probably pessimistically) that the whole scatter on repreated digitizings at one point on a perfect grid line is due to spot jitter. Thus

$$\sigma_{JITTER} = \sigma_{GRID\ LINE} = 0.61\ \mu m. \qquad (1)$$

When a bubble replaces the grid line the modulation depth of the video signal becomes smaller and the slope of the pulses less steep. Now electrical noise becomes significant:

$$\sigma_{BUBBLE} = \sqrt{\sigma^2_{SPOT\ JITTER} + \sigma^2_{NOISE\ BUBBLE}} \cdot \tag{2}$$

If a section of a track is scanned at 90° to the track direction, the total standard deviation is increased by the scatter of the bubbles about the track centre:

$$\sigma_{TRACK\ 90°} = \sqrt{\underbrace{\sigma^2_{SPOT\ JITTER} + \sigma^2_{NOISE\ BUBBLE}}_{\sigma^2_{BUBBLE}} + \sigma^2_{BUBBLE\ SCATTER}} \tag{3}$$

If a section of the track is scanned at 45° the total standard deviation is further increased. The scan lines do not in general pass exactly through the centre of each bubble and the track centre is found on a line perpendicular to the scan line direction as illustrated by the following sketch:

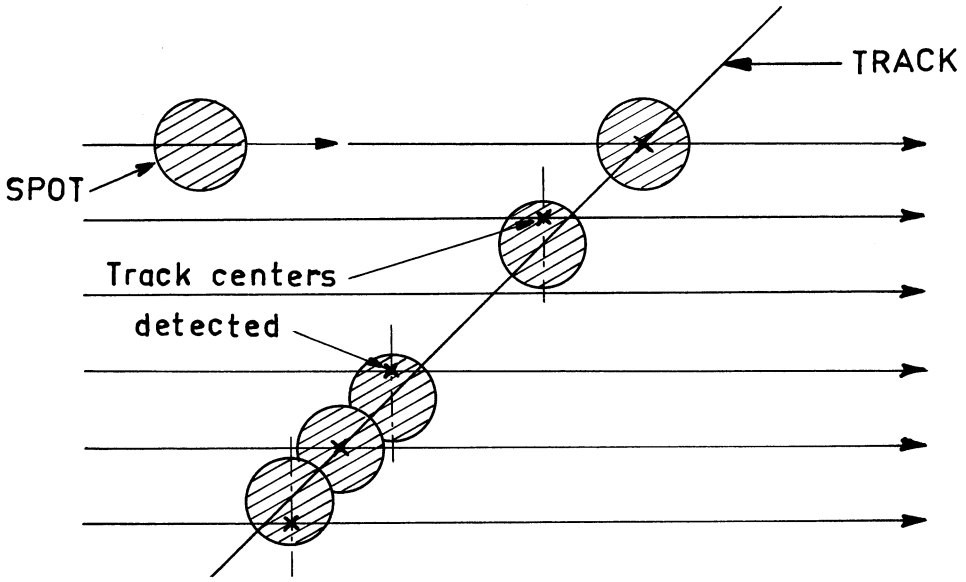

This scatter will be called $\sigma_{ERROR\ 45°}$. Using this term the total scatter at 45° is composed as follows:

$$\sigma_{TRACK\ 45°} = \sqrt{\sigma^2_{SPOT\ JITTER} + \sigma^2_{NOISE\ BUBBLE} + \sigma^2_{BUBBLE\ SCATTER} + \sigma^2_{ERROR\ 45°}} \tag{4}$$

From the Eqs. (2) to (4) the individual contributions can be calculated

successively using the measured values listed in Fig. 2 and repeated in the first column of Fig. 11.

From Eq. (2)

$$\sigma_{\text{NOISE BUBBLE}} = \sqrt{1.3^2 - 0.61^2} = 1.15 \text{ μm} . \qquad (2')$$

From Eq. (3)

$$\sigma_{\text{BUBBLE SCATTER}} = \sqrt{2.4^2 - 0.61^2 - 1.15^2} = 2.0 \text{ μm} . \qquad (3')$$

From Eq. (4)

$$\sigma_{\text{ERROR } 45^\circ} = \sqrt{3.7^2 - 0.61^2 - 1.15^2 - 2.0^2} = 2.8 \text{ μm} . \qquad (4')$$

Now Eqs. (2) to (4) can be used to extrapolate to other formats, scaling the spot jitter proportionally to the linear magnification and keeping the values found in Eqs. (2'), (3') and (4'), constant. The results of these calculations are listed in Fig. 11.

Three formats were examined:

i) 70 × 70 mm by which large chambers can be covered if the possibility of displacing the film gate is used.

ii) 70 × 115 mm to cover the BEBC photos.

iii) 50 × 130 mm covering the total area of the CERN 2m HBC.

As an example, $\sigma_{\text{TRACK } 90^\circ}$ in the 50 × 130 mm^2 format is calculated as follows using Eq. (3):

$\sigma_{\text{SPOT JITTER}}$ = 1.6 μm [extrapolated proportionally to the format change from the measured value 0.61 μm at 50 × 50 mm^2].

$\sigma_{\text{NOISE BUBBLE}}$ = 1.15 μm [calculated in Eq. (2') and assumed to remain constant].

$\sigma_{\text{BUBBLE SCATTER}}$ = 2.0 μm [calculated in Eq. (3') and assumed to remain constant].

Thus $\sigma_{\text{TRACK } 90^\circ \atop (50 \times 130)} = \sqrt{1.6^2 + 1.15^2 + 2.0^2} = 2.8 \text{ μm} .$

7. Estimation of the scanning speed for BEBC pictures

Both the low contrast of the picture and the smaller size of the bubble image will reduce the modulation of the photomultiplier signal. In order to maintain the original signal-to-noise ratio, the light intensity has to be increased correspondingly or the scanning speed and the bandwidth of the video amplifier reduced.

The contrast of bubble images on 2m HBC pictures is about 0.6. On BEBC pictures 0.3 is expected. This will decrease the modulation by $10^{(0.6-0.3)} = 2$. The ratio of the bubble image sizes is 25 μm: 8 μm*. Since (as a first approximation) the modulation varies as spot area, a reduction of modulation of $(25/8)^2 = 9$ can be expected. This gives a total reduction factor of $2 \times 9 = 18$.

The optical aperture on the CRT side of the lens during the tests was 1:16. Using a lens with a relative aperture of 1:2.8 and a demagnification of 1:0.7 results in a corresponding aperture of 1:6.8. The increase in light flux is $(16/6.8)^2 = 5.5$.

The remaining factor of 18:5.5 = 3.3 must be compensated by a corresponding reduction in scanning speed.

This leads to a scanning speed of 14 μm/μsec:3.3 = 4.2 μm/μsec.

8. Comparison of the phosphors type A and Q4

As mentioned before, two tubes of the same type (Ferranti 7/75 gun) have been used to compare the phosphors A and Q4. In Fig. 12 the properties of the two phosphors are compared.

Spot size: The spot size is measured at half amplitude using our 2-slit spot analyser. On the phosphor A the spot size was found to be as small as 13 μm, whereas on phosphor Q4 only 17 μm could be achieved. It seems that the screen material still increases the spot size since it can be assumed that the diameter of the electron beam is the same in both tubes. From a private communication from the PEPR Group in Oxford we know that the spot on a 9" tube with a phosphor Q4 has practically the same size as on our 7" tube. In both cases it was possible to maintain the original

---

* Note that 8 μm is the minimum expected image diameter for bubbles which are in the remote corners of the visible region in BEBC.

spot size all over the screen by applying dynamic corrections of focus and of astigmatism. Since

$$\frac{7"}{9"} \approx \frac{13\ \mu m(A)}{17\ \mu m(Q4)}$$

the relative resolution of both tubes is equivalent.

The phosphor noise of the phosphor A is 30% smaller than that of the phosphor Q4 (16% as against 22%) as shown in Fig. 13. Figures 14a and 14b give an idea of how much the phosphor noise can be compensated by using a reference photomultiplier looking at the screen: Fig. 14a shows the oscillogram of the photomultiplier signal, generated from a scan about 15 mm long across the calibration grid. In Fig. 14b the same signal is shown, but the part which is marked in the trace above is expanded in the pictures underneath.

Resistance against burning and fading: This point is considered to be rather important. For the Q4 phosphor, if a raster scan is repeated over the same area, the light output is reduced by up to 40%. The screen partly recovers ("fading"), but there is also a permanent reduction of light output ("burning"). This effect is particularly disadvantageous if raster scans partially overlap or certain areas are much more often scanned than others; e.g. areas where fiducial marks are situated. This effect is much less pronounced for the A phosphor.

Decay time: The disadvantage of the phosphor A is its longer decay time. But this difference is not as big as normally assumed. The characteristics of the rise and decay times of the phosphors A and Q4 are compared in Fig. 15. The curves are taken from the Ferranti catalogue, combining both curves. Comparing the curves one finds:

i) The rise and decay times are symmetrical.

ii) The decay time of the phosphor A decreases with increasing screen loading, whereas the characteristic of Q4 is independent of the screen loading. At high screen loading phosphor Q4 is only three to four times faster than phosphor A. High screen loading is used in our application as we are driving the screen into saturation.

These two properties allow electrical compensation of the rise and decay times, which has been used for several years in Luciole with success.

Resolution: Figures 16 and 17 show that at scanning speeds of up to about 10 µm/µsec the resolution of both tubes is about the same. In fact one should expect a higher modulation depth from the tube with phosphor A since the spot is smaller than that of the tube with phosphor Q4 (13:17). That this is not so is due to the longer decay time of the A phosphor. The extent to which this can be compensated for electrically is a function of light intensity. In our tests an aperture of 1:16 was used. A larger aperture would permit stronger compensation resulting in the same signal-to-noise ratio.

Price of lenses: Another advantage of phosphor A is that there are available for it high quality lenses whose price is only 2/3 of that for those offered for the Q4 spectrum ($\sim$ ₰ 3300 compared with $\sim$ ₰ 5000).

Selection of the phosphor: The disadvantage of longer decay time of the A phosphor becomes even less significant in the case of measuring BEBC pictures where the scanning speed has to be reduced to about 5 µm/µsec for reasons of signal-to-noise ratio as explained above. This, together with the other arguments in favour of a 7" phosphor A tube has lead us to the decision to use this tube.

9. Practical tests

The next two figures show practical results achieved with the phosphor A.

In Fig. 18 perfect dark lines on a transparent background have been scanned. In this case even lines of 1 µm could be vaguely detected.

In Fig. 19 very low contrast transparent lines on grey background have been scanned. This is to simulate the low contrast tracks of BEBC. Tracks having a contrast of 0.3 are very well detected. However, it is not astonishing that the track detection starts to fail at a contrast of 0.12.

Figure 20 allows a comparison of typical photomultiplier pulses generated by crossing tracks on 2m HBC film, normally developed and reverse developed. The better signal-to-noise ratio of the reverse developed film is obvious.

Figure 21 gives an idea of the extent to which faster scanning speeds can be used for display purposes. In the upper row phosphor A is used. For comparison the result obtained with Q4 and a spot size of 17 μm is shown for a speed of 100 μm/μsec.

Figure 22 shows what LUCY can detect from a low contrast track chamber picture. It represents the centre region of one of the first photos of the 1 m BEBC model. In this case phosphor Q4 was used, having a larger spot size than phosphor A.

Figure 23 presents the digitizings of tracks from a CERN 2 m HBC picture. In the first row the measured part of the original is shown. The second row shows the digitizings produced by HPD II at CERN and the third row the LUCY digitizings. Comparing rows 2 and 3 it is qualitatively obvious that the resolution of LUCY is as good as that of an HPD.

Figure 24 differs from Fig. 23 only in row 2 where for the LUCY digitizings the pulse width is plotted in addition to the centre position. This picture shows the possible use of the width information in confused areas.

Figure 25 gives an impression of the optical bench, the tube mount, the lens, the film gate and the film transport. The cover for the optical projection onto the screen is mounted above the optical bench.

10. Conclusions

From the results of the over-all measurements it can be concluded that the aim of constructing a CRT measuring system for bubble chamber pictures having a resolution and a stability comparable to that of an HPD has been achieved. Following the extrapolation of the results obtained on a 50 × 50 mm^2 area, it does not even seem to be necessary to measure the pictures of BEBC and of the 2 m HBC in sections of square format which

are measured separately by displacing the film stage as was originally conceived.

Two identical 7" cathode ray tubes type Ferranti 7/75 were examined, one with phosphor A, another with phosphor Q4. It was found that the resolution of the A tube is 30% better than that of the Q4 tube which must have a 9" screen to give the same value. The disadvantage of a longer decay time is compensated by other advantages at the scanning speeds of interest.

Calculations and tests show that it will be possible to detect and measure tracks in the photos from the large bubble chambers, such as BEBC.

Acknowledgements

The authors would like to thank Drs. J. Mayer and E. Quercigh for their continuous encouragement during this work.

They express their gratitude to Mr. G. Chanel and Mr. N. Damoiseau who have designed all the mechanical parts of LUCY with great care.

The authors have also very much appreciated the help of Mr. E. Riipinen*) in programming the calculations on the measurements. Mr. L. Sohet and Mr. H. Masuch have made very valuable contributions to the electronics.

---

*) On leave from the Department of Nuclear Physics, University of Helsinki, Finland.

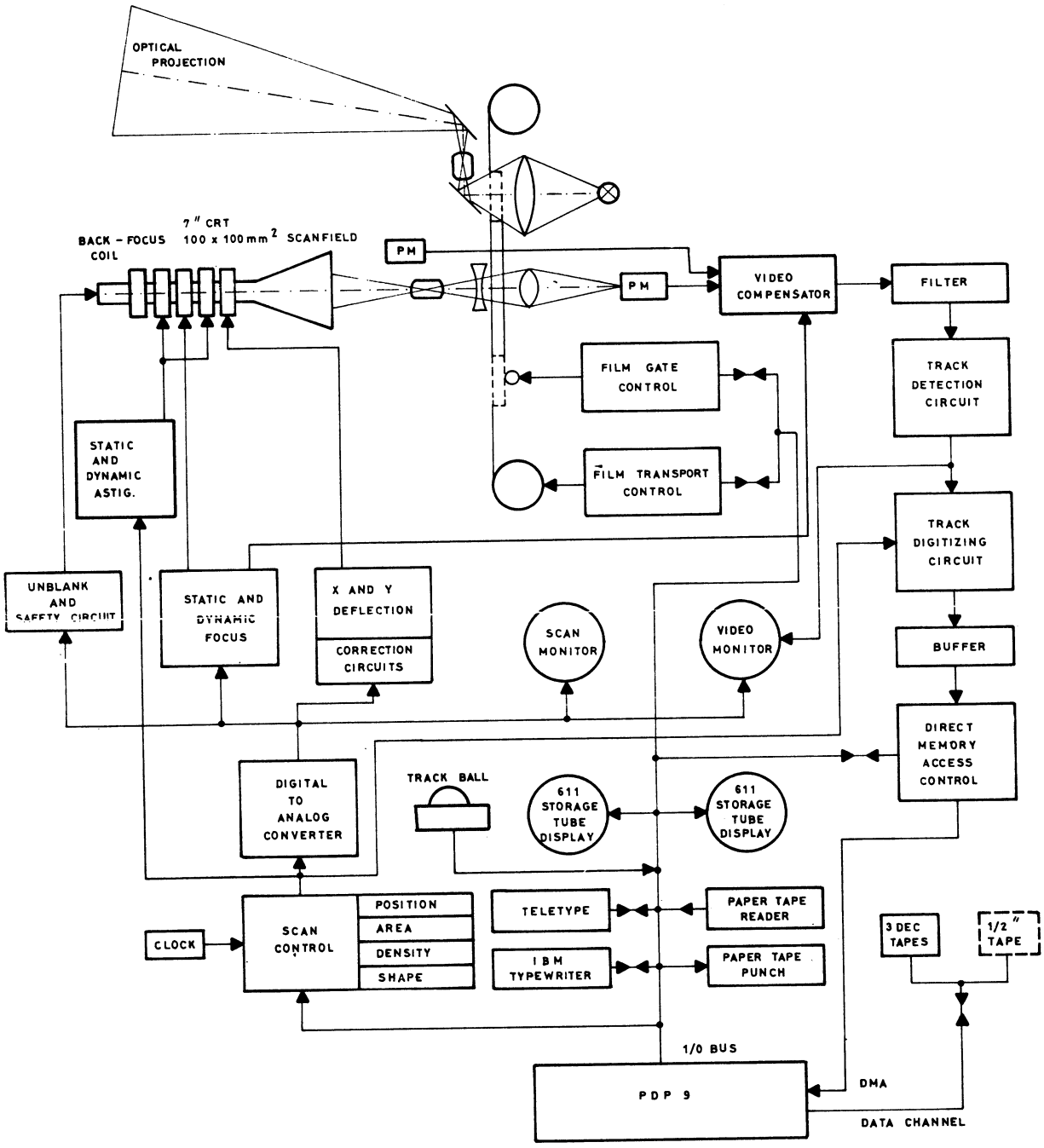

LUCY BLOCK DIAGRAM

FIG. 1

SUMMARY OF THE OVERALL TEST – SPOT UNDER DIGITAL CONTROL

PHOSPHOR Q4 – EFFECTIVE APERTURE 1:16
IN THE FILM PLANE: SPOT SIZE: 17 μm (CENTER), 24 μm (RASTER EDGES)
SPEED 14 μm/μs – SCAN AREA 50 x 50 mm^2 – LEAST COUNT 0.75 μm (1:65 000)

		FIG.
REPRODUCIBILITY OF INDIVIDUAL DIGITIZINGS: ON A GRID LINE	σ = 0.61 μm (< 1 l.c.)	3
REPRODUCIBILITY OF INDIVIDUAL DIGITIZINGS: ON A 2m HBC TRACK	σ = 1.3 μm	4
SCATTER OF DIGITIZINGS OF A TRACK OF ~8 mm LENGTH CERN 2m HBC: 90°	σ = 2.4 μm	5
SCATTER OF DIGITIZINGS OF A TRACK OF ~8 mm LENGTH CERN 2m HBC: 45°	σ = 3.7 μm	5
SCATTER OF DIGITIZINGS OF A LONG HORIZONTAL TRACK 2m HBC AFTER 5th ORDER FIT AND FILTERING	σ = 3.1 μm	6
SCATTER OF DIGITIZINGS ON 64 CALIBRATION CROSSES EVENLY DISTRIBUTED OVER THE SCANNING AREA	σ = 2 μm	7
LONG TERM STABILITY: DISPLACEMENT OF CALIBRATION CROSSES DURING 16 HOURS (PEAK-TO-PEAK VALUES)	5 μm p.p. (INSIDE MEASURING ERROR)	8
LARGE JUMP FROM EDGE TO CENTER, SETTLING TIME TO TWO LEAST COUNTS PRECISION	250 μs	
PRELIMINARY CALIBRATION	SEE FIG.	9

FIG. 2

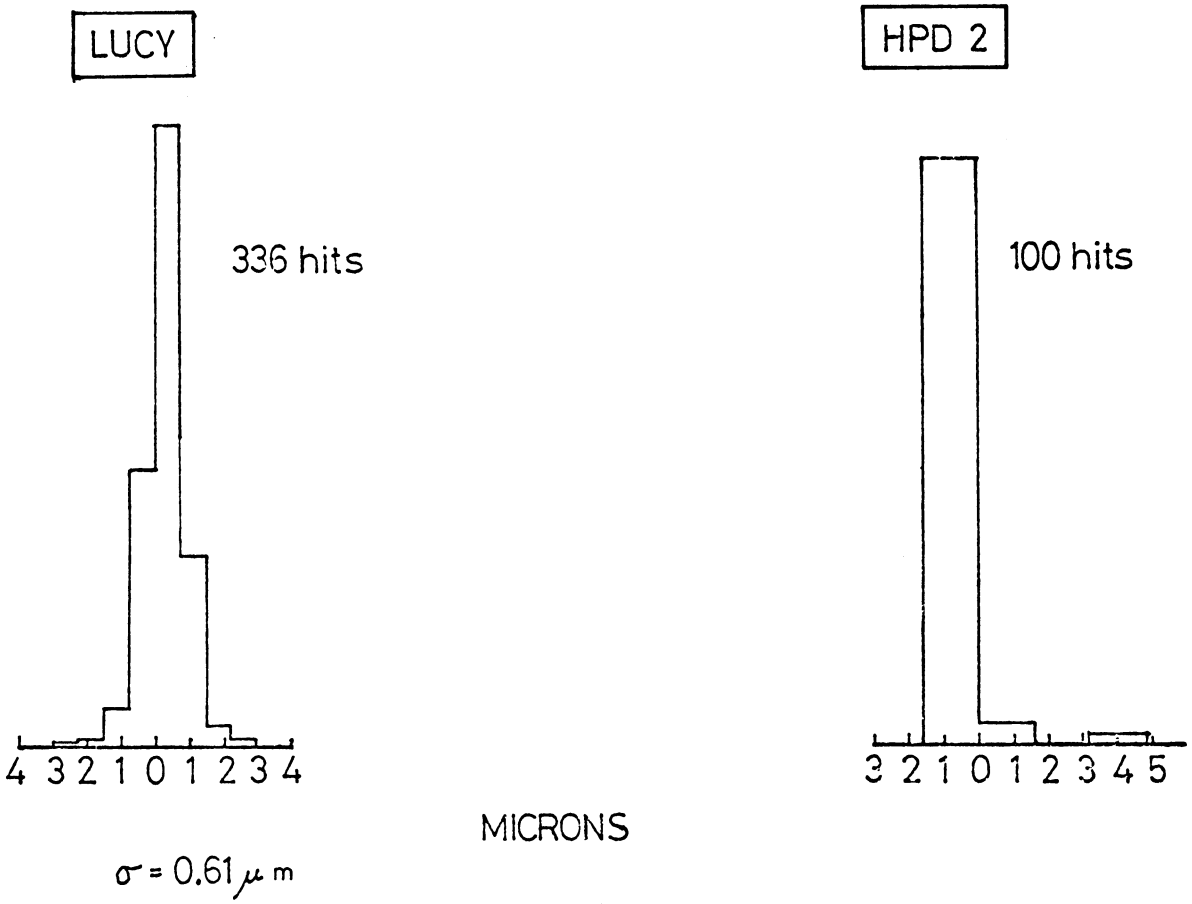

REPRODUCIBILITY OF INDIVIDUAL DIGITIZINGS

30 MICRON GRID LINE NORMAL TO SCAN DIRECTION

FIG. 3

LUCY

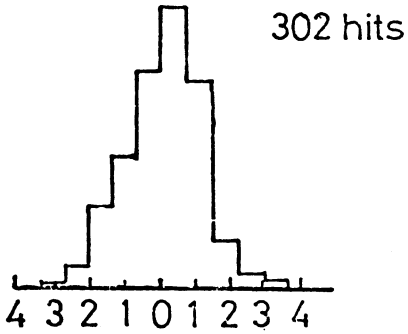

$\sigma = 1.3 \mu m$

REPRODUCIBILITY OF INDIVIDUAL DIGITIZINGS

CERN 2m H BC TRACK AT 90°

FIG. 4

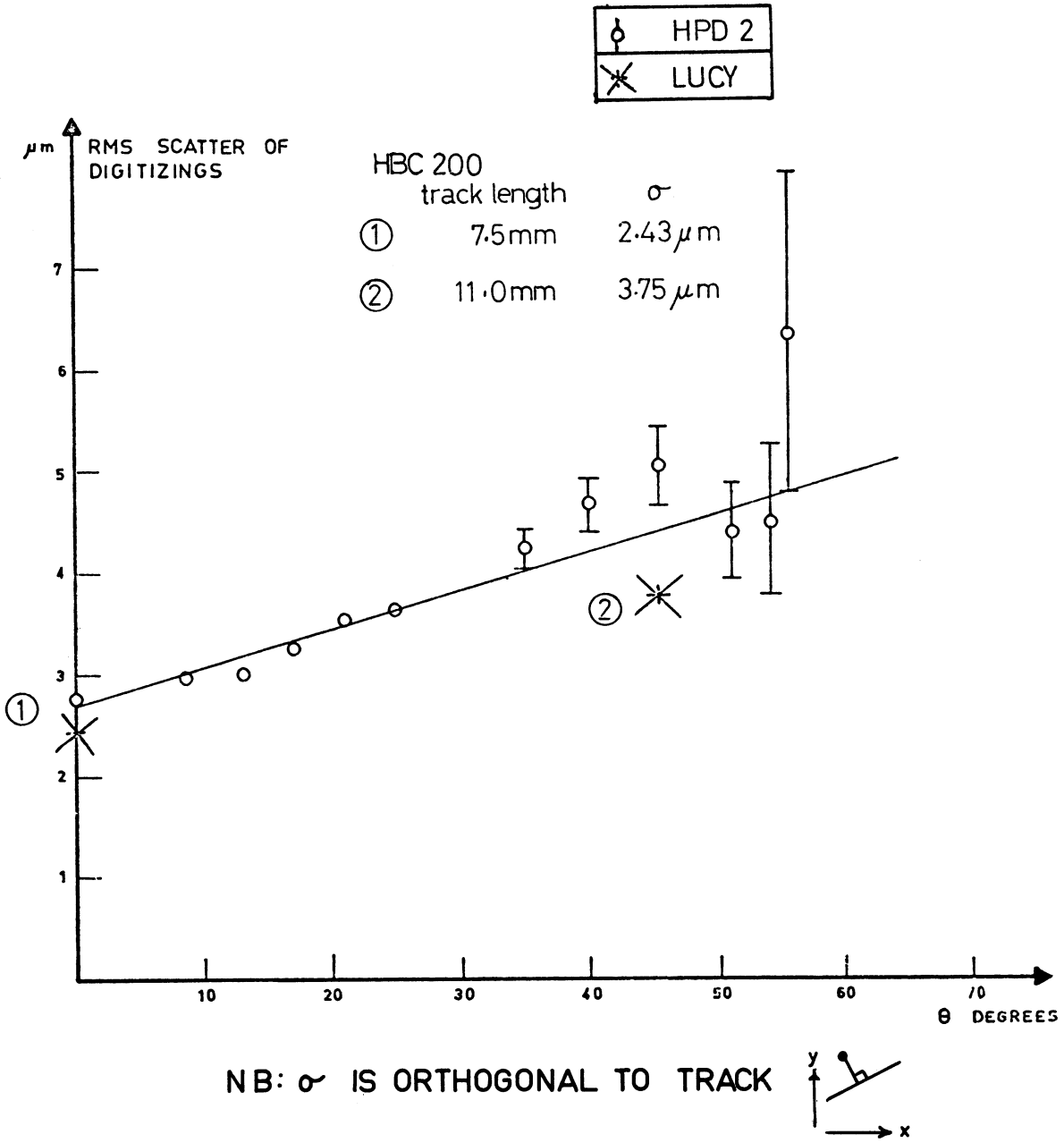

SCATTER OF THE DIGITIZINGS ALONG A TRACK AS A FUNCTION OF THE ANGLE WITH THE SCANLINE

THE VALUES ① AND ② MEASURED ON LUCY ARE ADDED TO THE DIAGRAM OF HPD II FOR COMPARISON (SEE CERN REPORT NO 68-4)
THE σ LUCY IS DETERMINED BY A 5^{TH} ORDER POLYNOMIAL FIT TO THE RAW DIGITIZINGS WITH NO FILTERING.

FIG. 5

FITTING PROCESS:

1. 2^{nd} ORDER FIT TO ALL DIGITIZINGS	σ = 40 μm
2. REJECT ALL DIGITIZINGS WITH RESIDUALS > 2 σ	
3. 5^{th} ORDER FIT TO REMAINING DIGITIZINGS	σ = 4.05μm
4. REJECT ALL DIGITIZINGS WITH RESIDUALS > 2 σ	
5. 5^{th} ORDER FIT TO REMAINING DIGITIZINGS	σ = 3.08 μm

TRACK LENGTH : 35 mm
SCANNING DIRECTION : VERTICAL
SCAN LINE SPACING : 25μm
SCAN LINE LENGTH : 770μm

NO HARDWARE FILTERING, NO WIDTH SELECTION

SCATTER OF THE DIGITIZINGS OF A LONG HORIZONTAL TRACK IN THE CERN 2m HBC

FIG. 6

8 x 8 INTERSECTIONS OF THE CALIBRATION GRID, EVENLY DISTRIBUTED OVER THE SCAN AREA (SEE FIG. 9) WERE EACH COVERED BY A HORIZONTAL RASTER OF $4 \times 4\ mm^2$

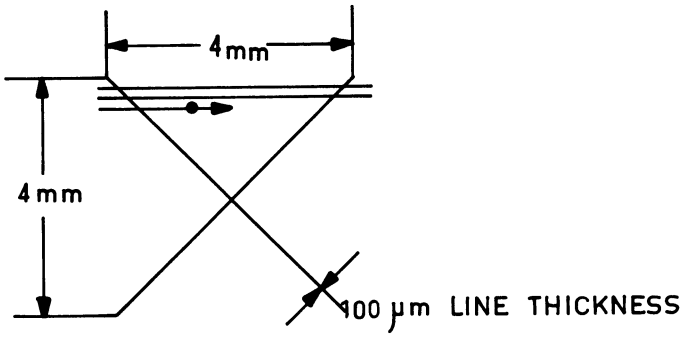

A STRAIGHT LINE WAS FITTED TO EACH ARM OF THE CROSSES.

SCATTER OF THESE DIGITIZINGS OVER THE WHOLE AREA

$$\sigma \lesssim 2\mu m$$

SCATTER OF THE DIGITIZINGS OF CALIBRATION MARKS AT VARIOUS POSITIONS AT THE SCREEN

FIG. 7

LONG TERM STABILITY

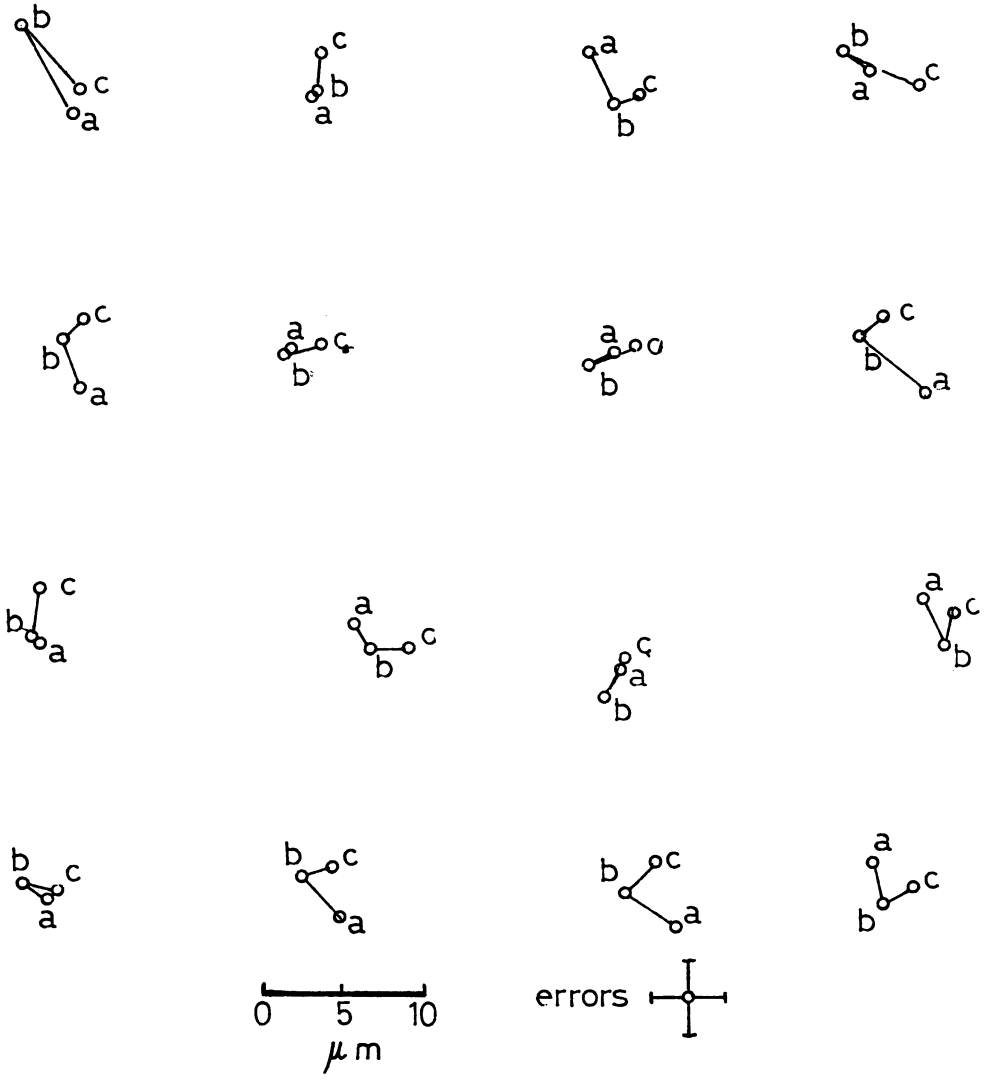

THE POSITION OF 16 FIDUCIAL CROSSES WAS MEASURED IN A PERIOD OF 16 HOURS.

	MEASUREMENT TIME
a	0 hr
b	0 + 1 hr
c	0 + 16 hr

THE DISPLACEMENT DOES NOT EXCEED THE MEASURING ERROR, WHICH WAS HERE INCREASED TO 5μm r.m.s. BECAUSE THE SPOT WAS ACCIDENTALLY DEFOCUSSED TO 60μm ON THE FILM.

FIG. 8

PRELIMINARY CALIBRATION

DISTRIBUTION OF THE FIDUCIALS MEASURED

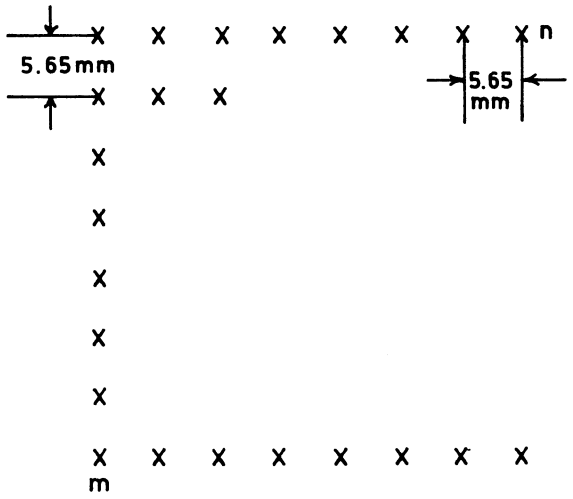

5th ORDER FIT WITH LOW ORDER WEIGHT ON THE CORNER FIDUCIALS:

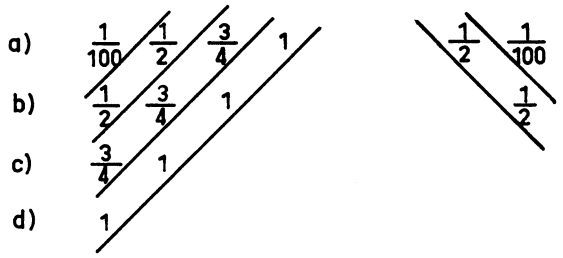

EXCLUDING FIDUCIALS a) (IN THE CORNERS)

σ_x = 2.9μm (MAXIMUM 8.8μm)
σ_y = 3.6μm (MAXIMUM 8.1μm)

WHERE

$$\sigma_x = \sqrt{\frac{\sum_{m,n} (X_{m,n} - X'_{m,n})^2}{NDF}}$$

$$\sigma_y = \sqrt{\frac{\sum_{m,n} (Y_{m,n} - Y'_{m,n})^2}{NDF}}$$

FIG. 9

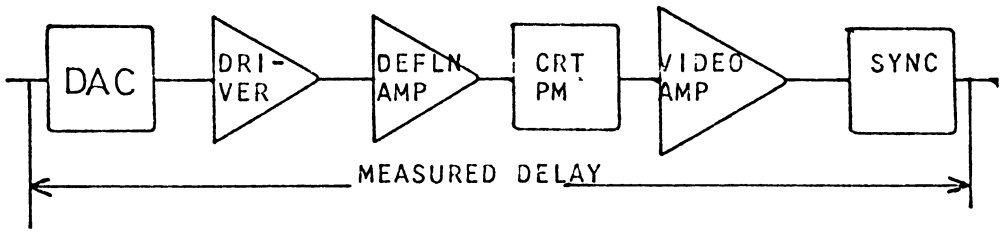

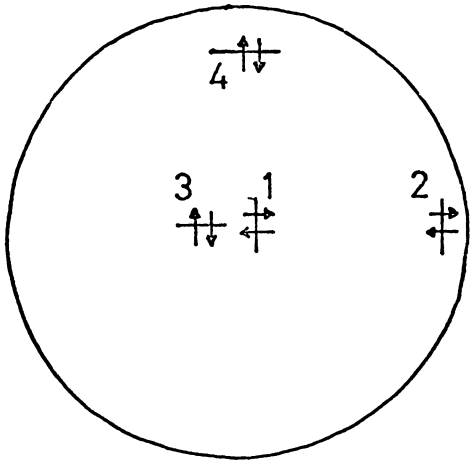

SWEEP SPEED 14 μm/μs

POSN	DIRN	DELAY TIME [μS]	EQUIV DIST [μm]
1	X	4.51 ± .04	63.1 ± 0.5
2	X	4.42	61.9
3	Y	4.40	61.6
4	Y	4.52	63.3

SCAN DELAY TIME AS A FUNCTION OF SCAN POSITION

FIG. 10

EXTRAPOLATION OF THE RESULTS FROM 50 x 50 mm^2 SCANNING AREA TO LARGER FORMATS

ASSUMPTION: 1. SPOT SIZE $<25\mu m$ IN THE USEFUL AREA
2. THE QUALITY OF THE TRACKS IS THE SAME IN ALL FORMATS

FORMAT	50 x 50	70 x 70	70 x 115	50 x 130	mm
UTILISATION	2m HBC / LARGE CHAMBERS — DISPLACING FILM GATE		BEBC	2m HBC	
LEAST COUNT	0.76	1.07	1.75	1.98	μm
REPRODUCIBILITY PERFECT LINE (σ_{JITTER})	0.61 (Fig.3)	0.85	1.4	1.6	σ IN μm
REPRODUCIBILITY SINGLE BUBBLE (σ_{BUBBLE})	1.3 (Fig.4)	1.4	1.8	2.0	
SCATTER ON TRACKS 90° ($\sigma_{TRACK\ 90°}$)	2.4 (Fig.5)	2.5	2.7	2.8	
SCATTER ON TRACKS 45° ($\sigma_{TRACK\ 45°}$)	3.7 (Fig.5)	3.8	3.9	4.0	
	MEASURED	EXTRAPOLATED			

FIG.11

SUMMARY OF THE MEASURING RESULTS — COMPARISON BETWEEN PHOSHORS

TUBES: FERRANTI 7"/75 TETRODE

	PHOSPHOR A	PHOSPHOR Q 4	FIG.
SPOT SIZE (HALF AMPLITUDE)			
CENTER	13 µm	17 µm	
CORNER — DYNAMIC FOCUS	45 µm	45 µm	
CORNER (WORST CASE) — DYNAMIC FOCUS + ASTIGMATISM	13 µm	17 µm	
PHOSHOR NOISE (PEAK-TO-PEAK)	16 %	22 %	
RESISTANCE AGAINST BURNING AND FADING	GOOD	POOR	
RISE AND DECAY TIME TO 80 % RESP. 20 %	300 ns (AT HIGH SCREEN LOADING)	80 ns	15
ESTIMATED MAX. MEASURING SPEED			
HIGH CONTRAST TRACKS (2m HBC)	20 ··· 30 µm/µs	20 ··· 50 µm/µs	
LOW CONTRAST TRACKS (BEBC)	2.5 ··· 10 µm/µs	—	
PRICE OF AVAILABLE LENSES WITH COMPARABLE QUALITY	~ 3 300 ₰	~ 5 000 ₰	

FIG. 12

PHOSPHOR A

PHOSPHOR Q 4

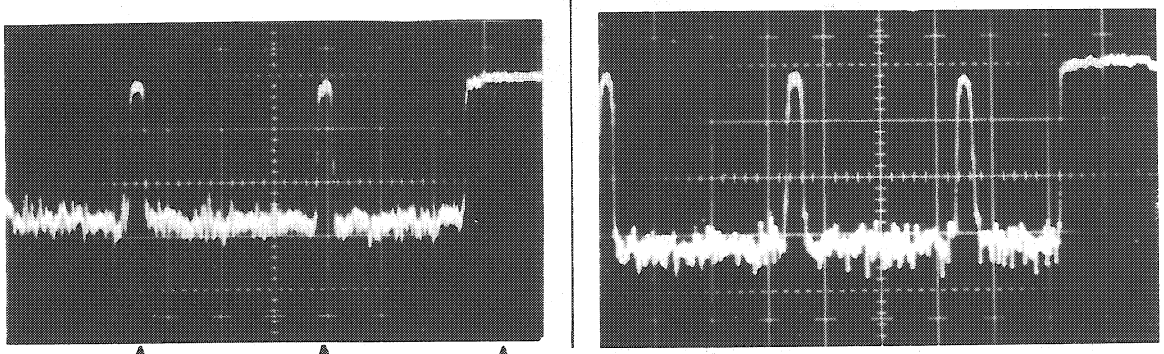

SPEED ON THE FILM 2.5 μm/μs

SIN^2 FILTER 3.3 μs

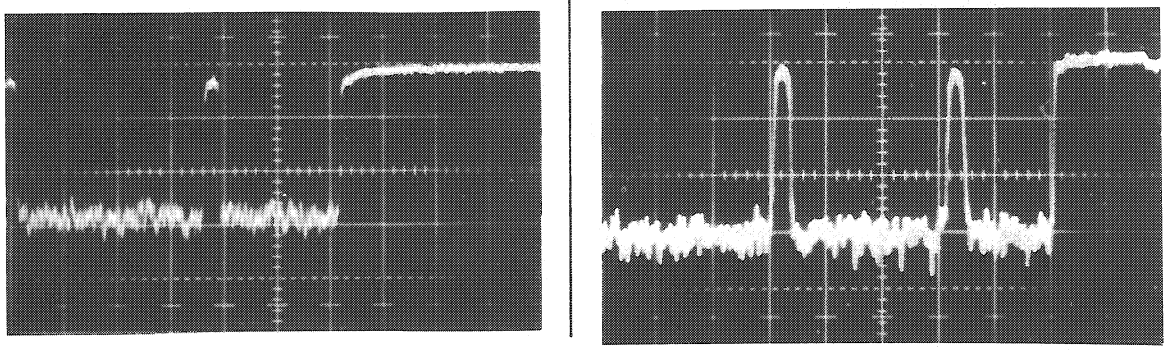

5μm/μs

FILTER 2.2 μs

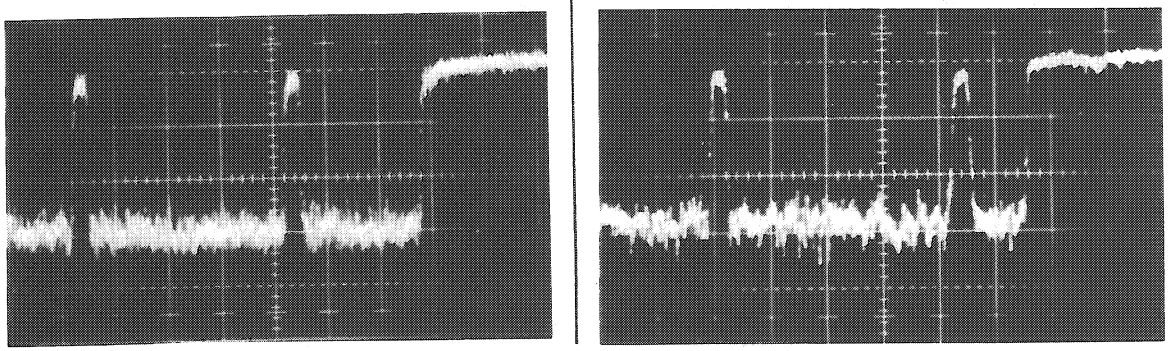

10μm/μs

FILTER 0.4 μs

SCREEN NOISE AT SCANNING SPEEDS 2.5 TO 10μm/μs AFTER APPROPRIATE ELECTRICAL FILTERING.

FIG. 13

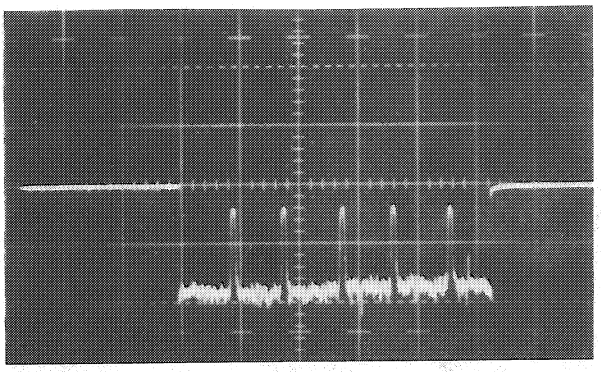

A) VIDEO SIGNAL

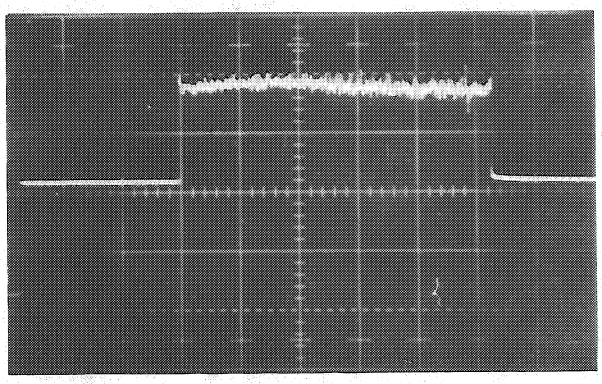

B) REFERENCE PHOTOMULTIPLIER SIGNAL

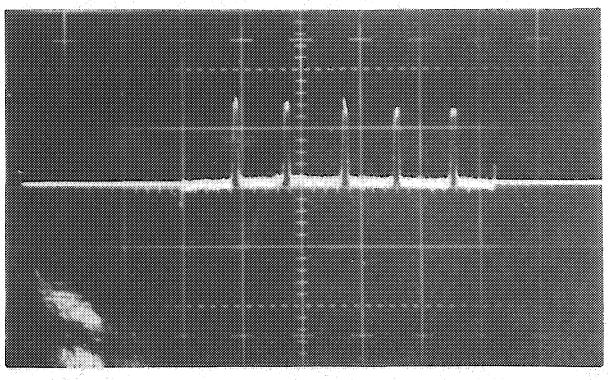

C) COMPENSATED VIDEO SIGNAL

COMPENSATION OF SCREEN NOISE I

PHOSPHOR Q 4

SCANNING SPEED 12 µm/µs

FIG. 14a

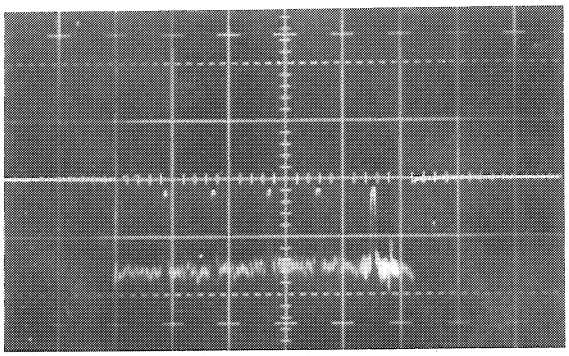

VIDEO SIGNAL

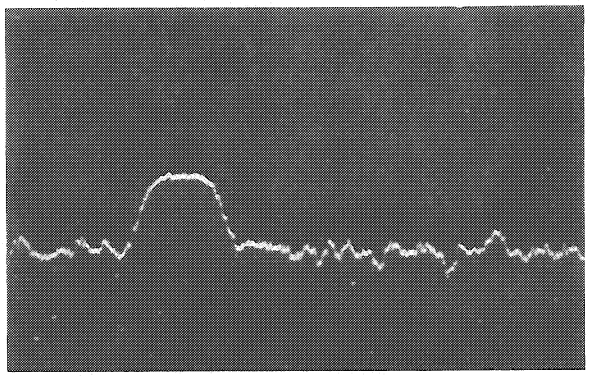

A) VIDEO SIGNAL EXPANDED

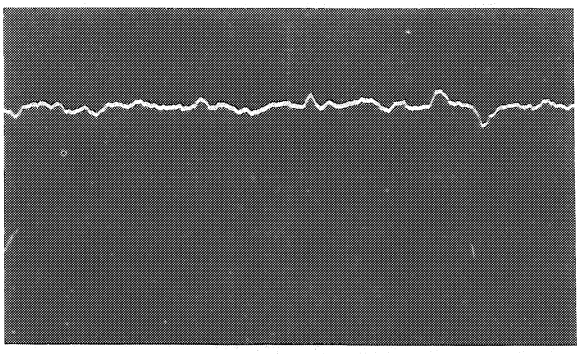

B) REFERENCE PHOTO-MULTIPLIER SIGNAL

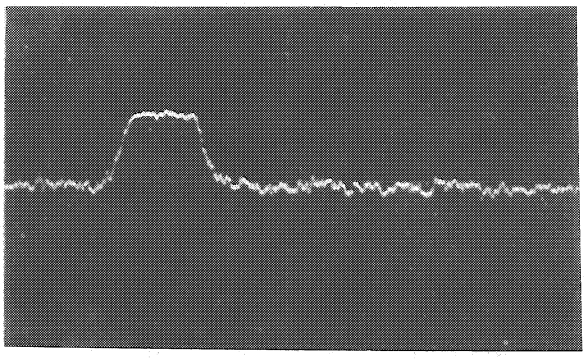

C) COMPENSATED VIDEO SIGNAL

COMPENSATION OF SCREEN NOISE II

FIG. 14 b

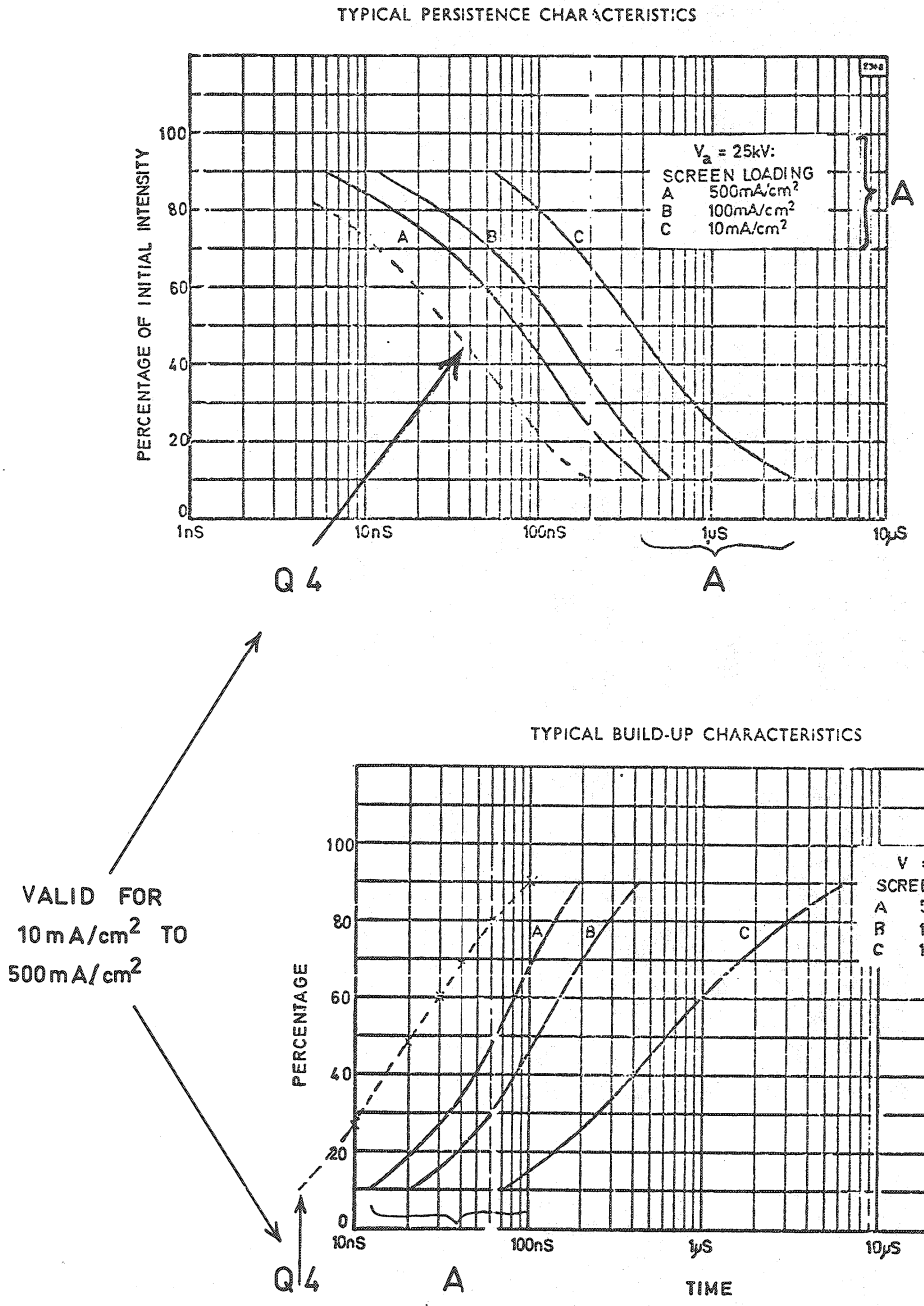

COMPARISON BETWEEN BUILD-UP AND PERSISTANCE CHARACTERISTICS OF THE PHOSPHORS Q4 AND A (FERRANTI)

1. RISE AND DECAY TIMES ARE NEARLY SYMMETRICAL
2. AT HIGH SCREEN LOADINGS THE TIMES FOR A ARE ONLY 3 TO 4 TIMES LONGER THAN FOR Q4.

FIG. 15

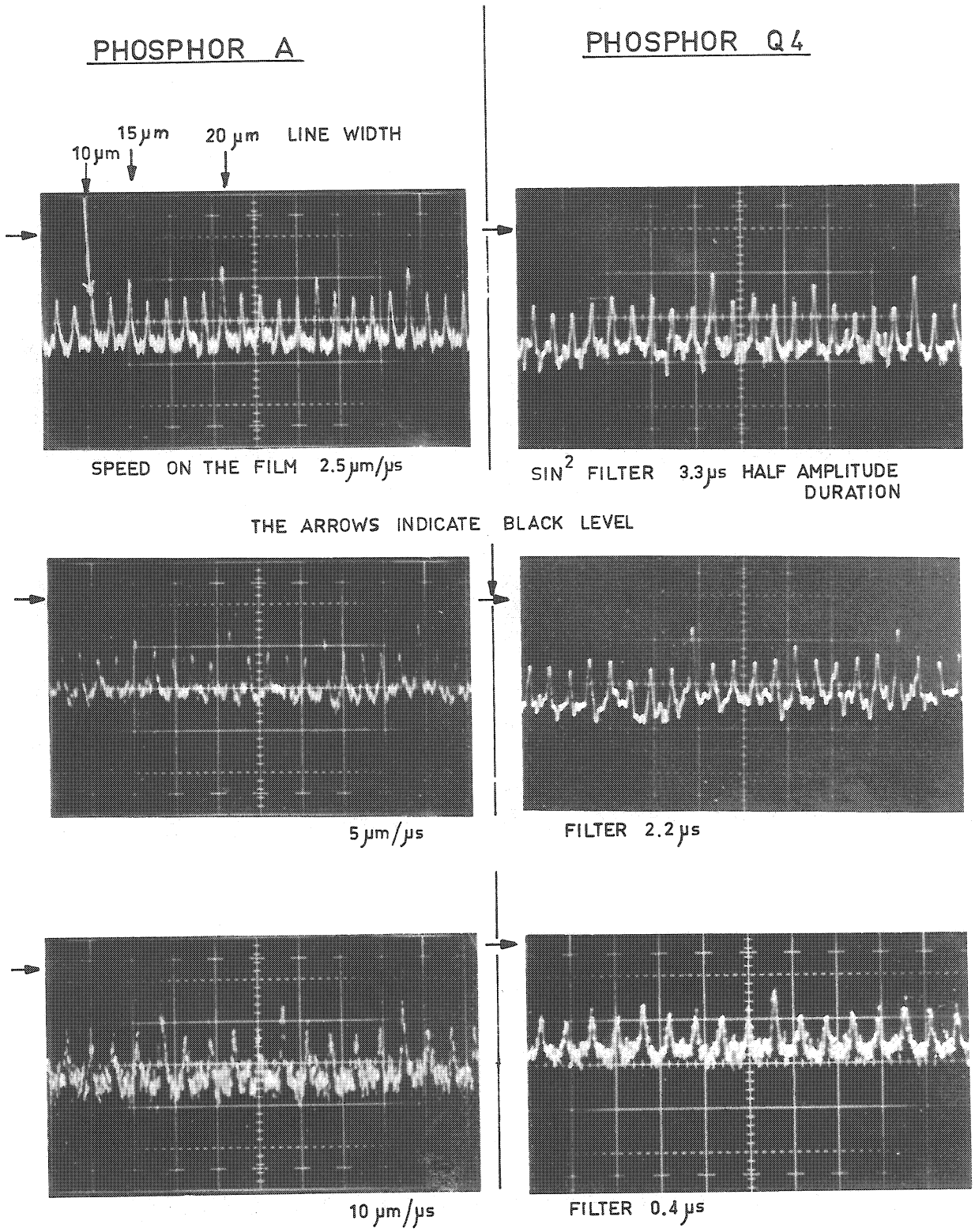

RESOLUTION TEST : BLACK LINES ON TRANSPARENT BACKGROUND 10µm, 15µm, 20µm

FIG. 16

PHOSPHOR A

PHOSPHOR Q4

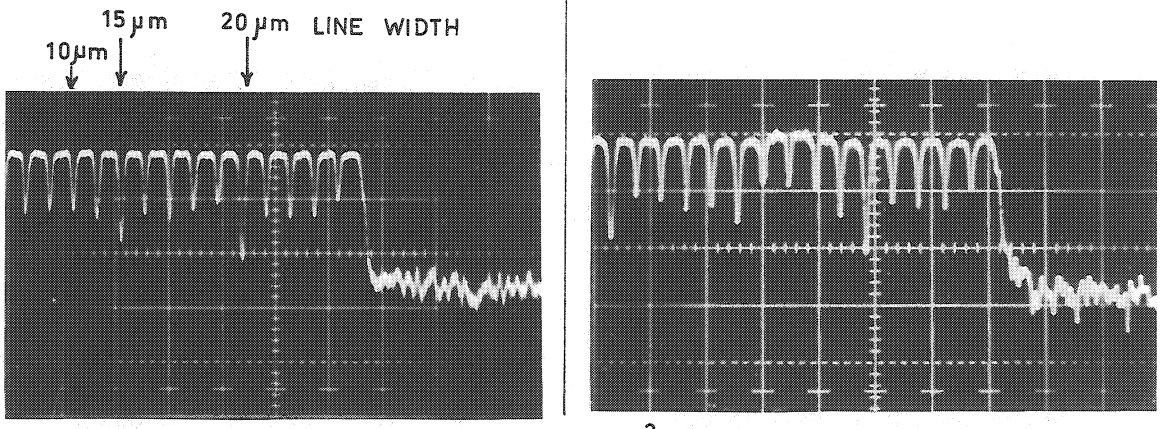

SPEED ON THE FILM 25 µm/µs

SIN^2 FILTER 3.3 µs

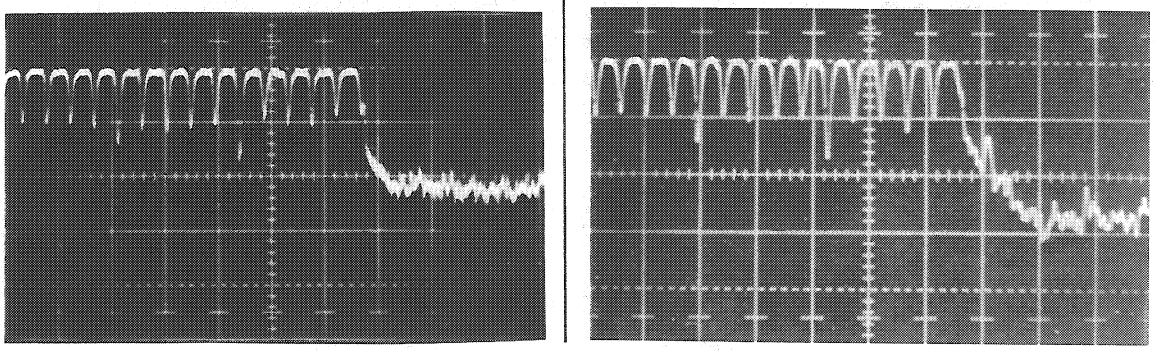

5 µm / µs

FILTER 2.2 µs

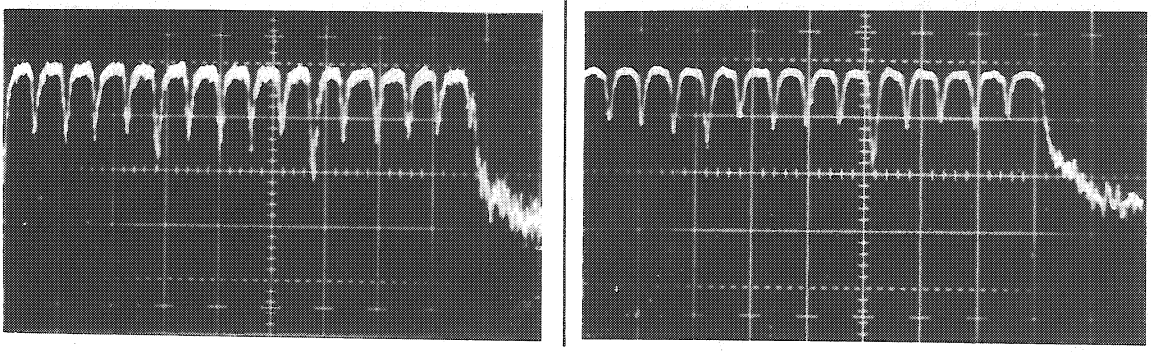

10µm / µs

FILTER 0.4 µs

RESOLUTION TEST: TRANSPARENT LINES ON DARK BACKGROUND
10 µm, 15 µm, 20 µm

FIG. 17

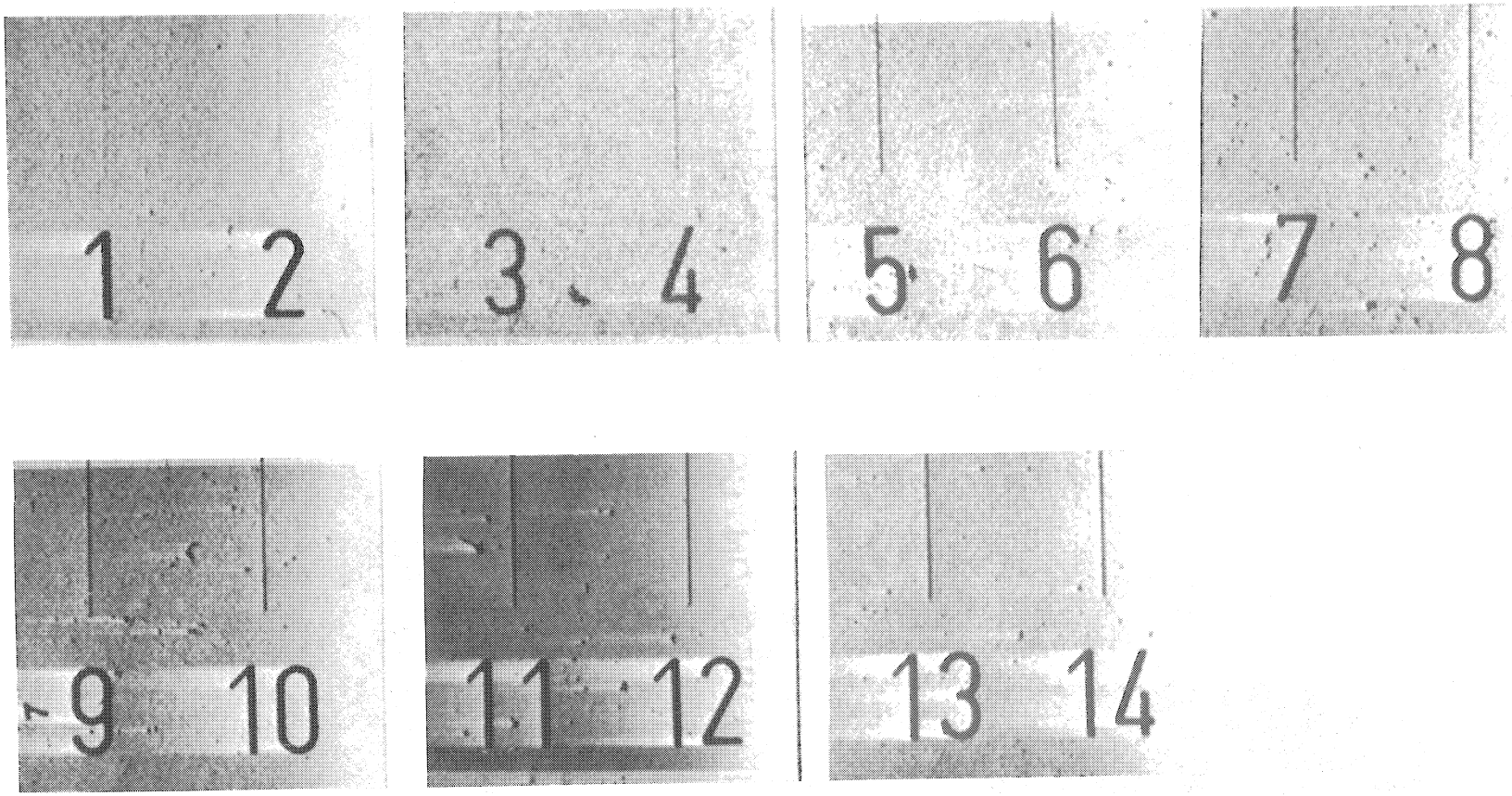

RESOLUTION TEST

PHOSPHOR A

IN THE FILMPLANE:

BLACK LINES ON TRANSPARENT BACKGROUND, THE LINE WIDTH IS INDICATED BY THE NUMBERS UNDERNEATH EACH LINE.

DISPLAY OF TRACKDETECTOR SIGNAL ON AN OSCILLOSCOPE SCREEN
SPOT SIZE 10 µm, SCANNING SPEED 5 µm/µs, SCAN LINE SPACING 20 µm

FIG. 18

PHOSPHOR A RESOLUTION TEST

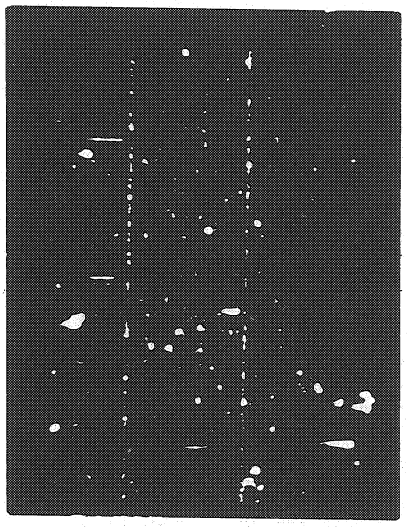

CONTRAST C = 0.12

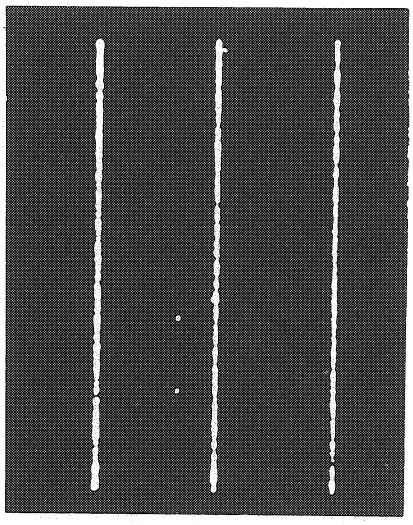

CONTRAST C = 0.35

TRANSPARENT LINES ON GREY BACKGROUND

LINE WIDTH 7 µm

TRACKDETECTOR OUTPUT DISPLAYED ON AN OSCILLOSCOPE SCREEN
IN THE FILMPLANE : SPOT SIZE 10 µm
SCANNING SPEED 5 µm/us
SCAN LINE SPACING 20 µm

FIG. 19

TYPICAL PULSES FROM 2 m HBC – FILM

SPOT SIZE ON THE FILM 10 µm
SCANNING SPEED 5 µm/µs ON FILM
SIN^2 FILTER 2.2 µm/µs H.A.D.

PHOSPHOR A

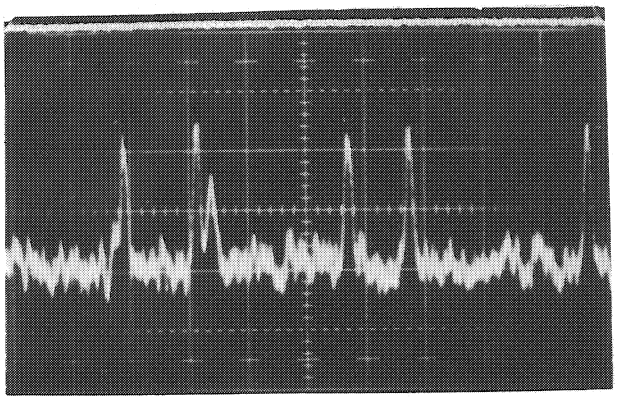

NORMAL DEVELOPMENT
BLACK TRACKS ON
TRANSPARENT BACK-
GROUND

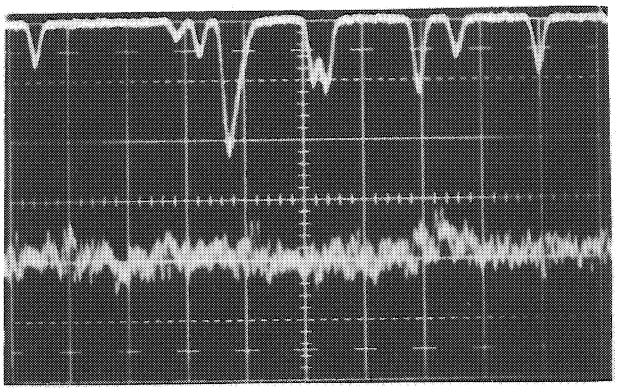

REVERSE DEVELOPMENT
TRANSPARENT TRACKS ON
BLACK BACKGROUND

PM Signal →
with out film,
for reference

FIG. 20

PHOSPHOR A SPOT SIZE 10 μm ON THE FILM

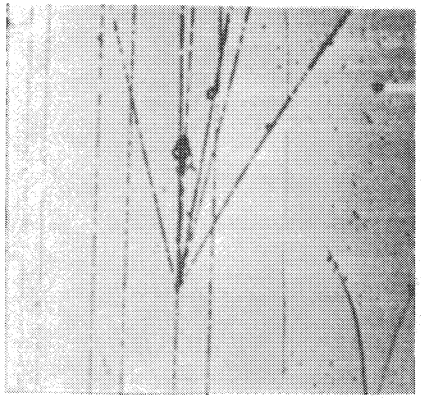

5 μm/μs

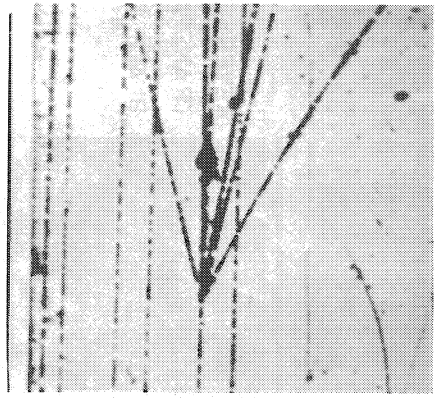

10 μm/μs

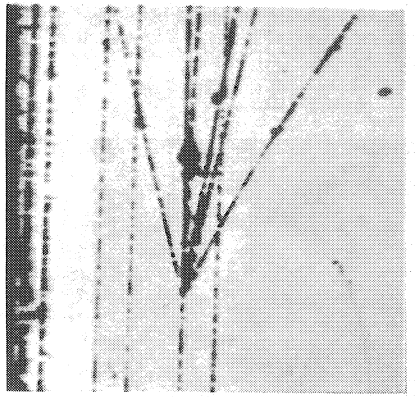

50 μm/μs

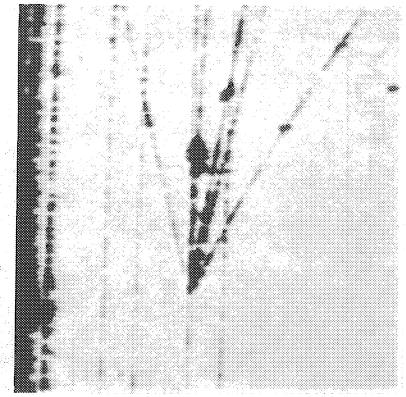

100 μm/μs

CERN 2m HBC PICTURES SCANNED AT VARIOUS SPEEDS AND DISPLAYED ON A CRT SCREEN

RASTER SCAN, DISTANCE OF LINES 20 μm
THE INTENSITY OF THE CRT IS CONTROLLED
BY THE OUTPUT OF THE TRACK CENTER CIRCUIT (BLACK–WHITE)

FIG. 21

PHOSPHOR Q4
SPOT SIZE 17 μm

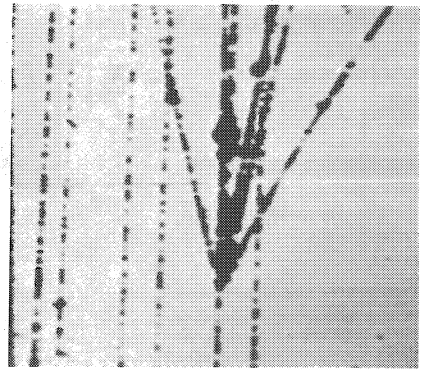

PHOSPHOR Q 4

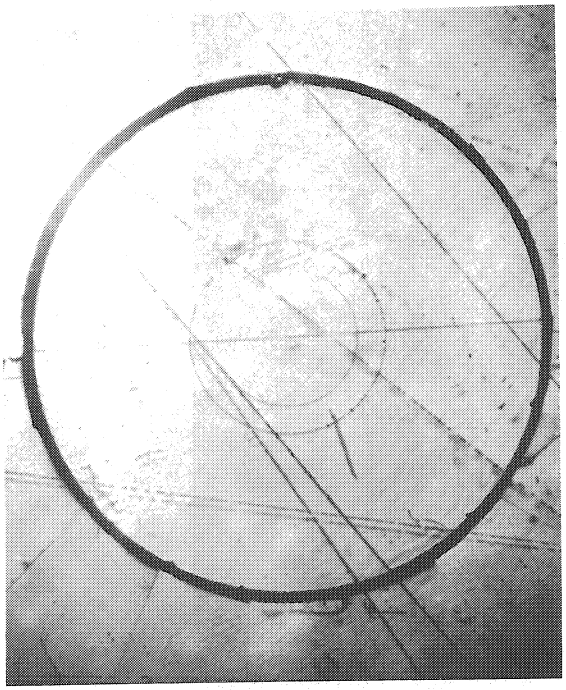

PART OF THE ORIGINAL

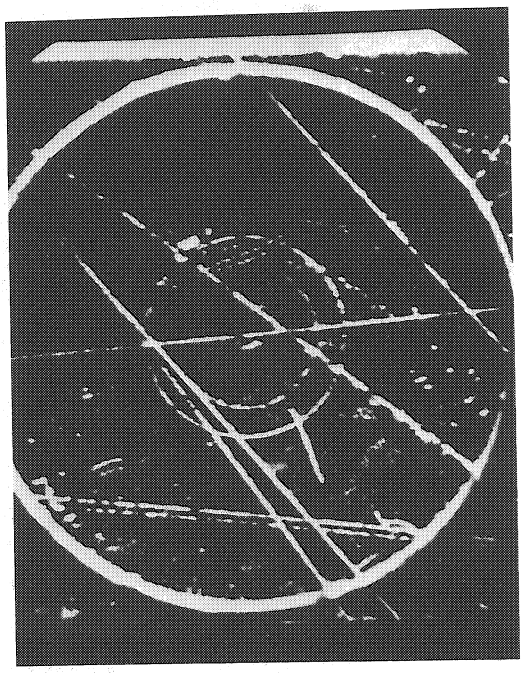

DISPLAY OF TRACKDETECTOR
OUTPUT ON A SCOPE

FILM OF BEBC MODEL

CONTRAST OF THE BUBBLE IMAGES ABOUT 0.3
IN THE FILMPLANE: SPOT SIZE 17 µm
SCANNING SPEED 10 µm/µs
SCAN LINE SPACING 20 µm/µs

FIG.22

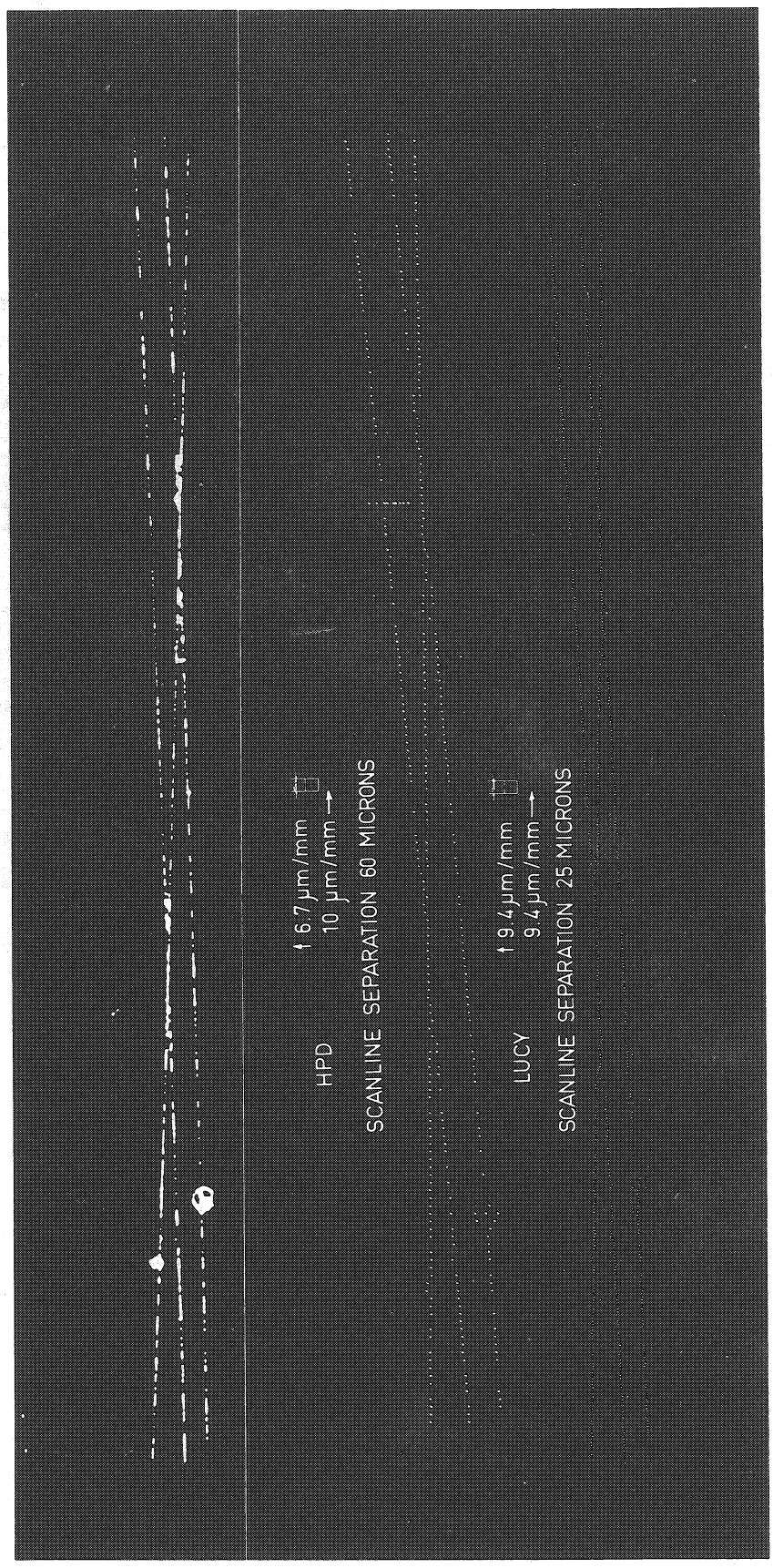
HPD
↑ 6.7 µm/mm
10 µm/mm →
SCANLINE SEPARATION 60 MICRONS
LUCY
↑ 9.4 µm/mm
9.4 µm/mm →
SCANLINE SEPARATION 25 MICRONS

FIG. 23

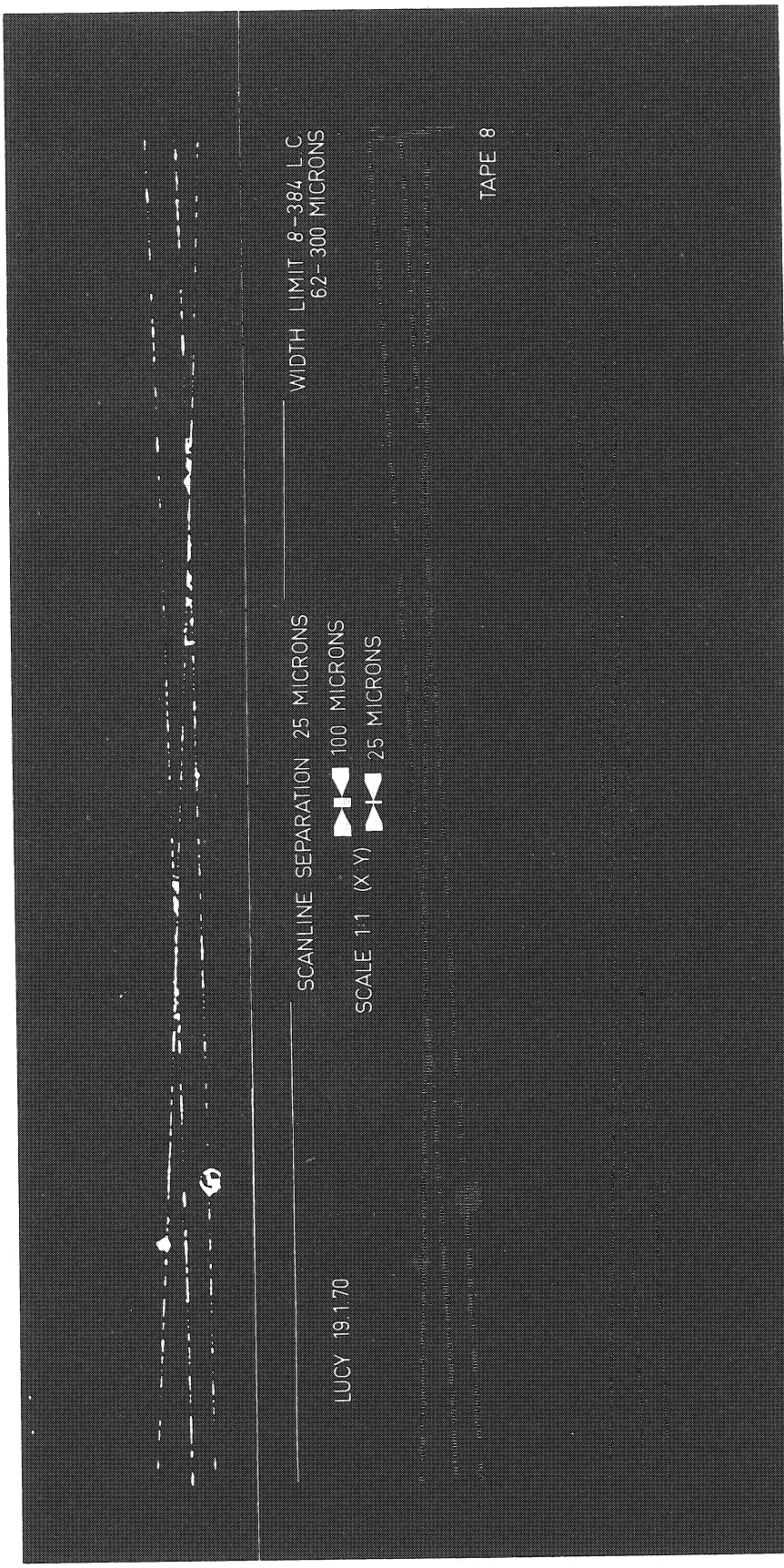
WIDTH LIMIT 8-384 L.C
6.2-300 MICRONS
SCANLINE SEPARATION 25 MICRONS
100 MICRONS
SCALE 1:1 (X Y)
25 MICRONS
LUCY 19.1.70
TAPE 8

FIG. 24

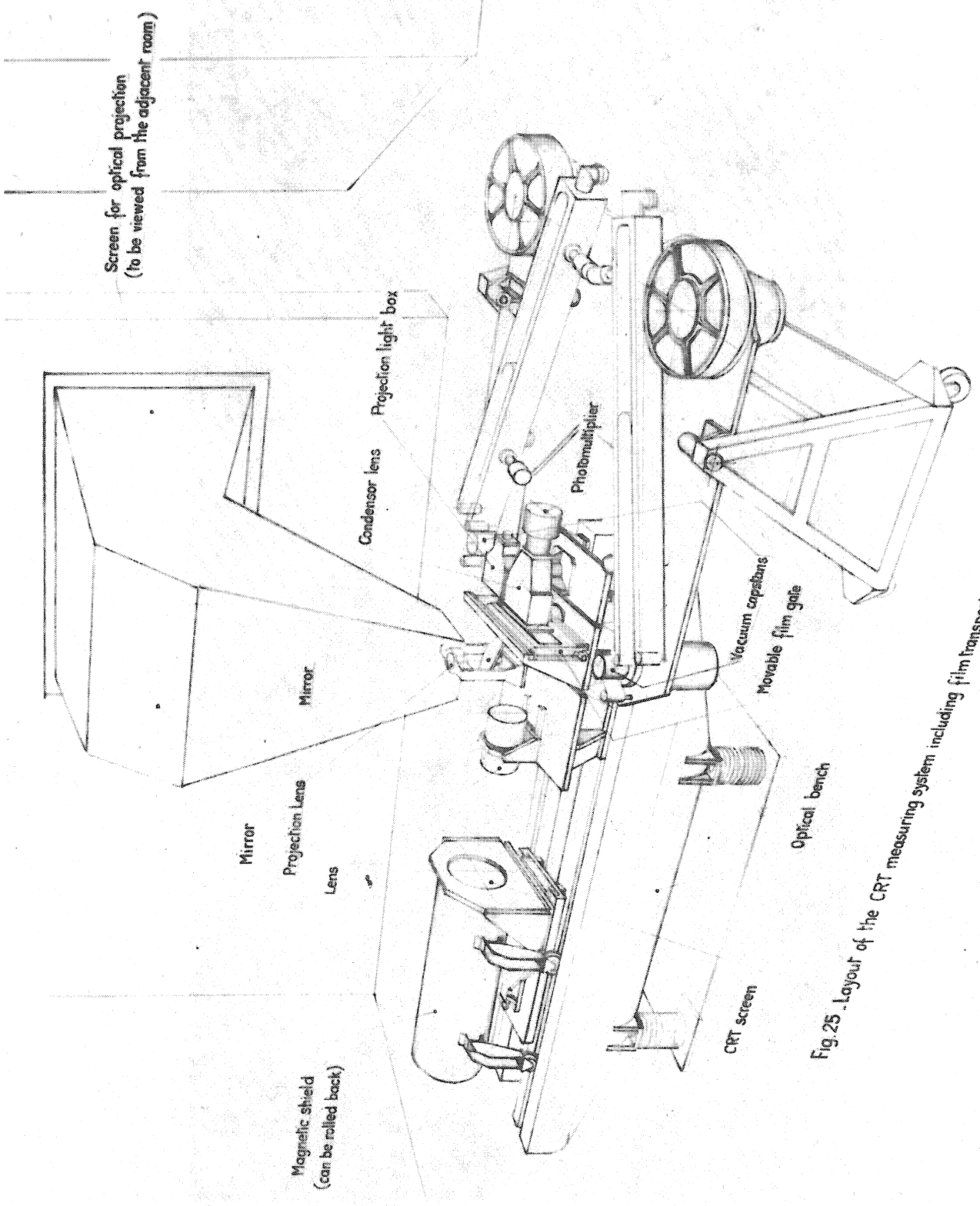

Fig.25 Layout of the CRT measuring system including film transport.